TITLE: A Method for Imaging the Ischemic Penumbra with MRI using IVIM

Authors: Mira M. Liu[1,2,*], Niloufar Saadat[3], Steven P. Roth[4], Marek A. Niekrasz[5], Mihai Giurcanu[6], Mohammed Salman Shazeeb[7], Timothy J. Carroll[1], Gregory A. Christoforidis[3,8]

[1]Department of Radiology Medical Physics, University of Chicago, Chicago, IL, USA

[2]Current affiliation: Biomedical Engineering and Imaging Institute, Icahn School of Medicine at Mount Sinai, New York, NY, USA

[3]Department of Interventional Radiology, University of Chicago, Chicago, IL, USA

[4]Department of Anesthesiology, University of Illinois, Chicago, IL, USA

[5]Department of Surgery and Large Animal Studies, University of Chicago, Chicago, IL, USA

[6]Department of Statistics, University of Chicago, Chicago, IL, USA

[7]Department of Radiology, University of Massachusetts Chan Medical School, Worchester, MA, USA

[8]Current affiliation: Radiology, Mount Carmel Health Systems, Columbus, OH, USA

(*)Correspondence:
Mira M. Liu

Icahn School of Medicine at Mount Sinai

BioMedical Engineering and Imaging Institute

1470 Madison Ave, 1st Floor

New York, NY 10029

Tel: (212) 824-8480

E-mail: mirabai.liu@mountsinai.org

Grant Support

The authors would like to acknowledge the support of the US National Institutes of Health R01-NS093908 (Carroll/Christoforidis) and The National Science Foundation DGE-1746045 (Liu).

Running Title: Local Perfusion in Ischemic Penumbra with IVIM

ABSTRACT

Purpose: In acute ischemic stroke, the volume and degree to which blood supply is reduced or compensated through collateral flow, in addition to time from symptom onset and NIH stroke scale, may include valuable information regarding the rate at which an infarct is expanding and treatment response. The purpose of this work was to test the hypothesis that intravoxel incoherent motion MRI (IVIM) can quantify local cerebral blood flow (qCBF), infarct volume, and define the ischemic penumbra for determination of the perfusion-diffusion mismatch (PWI/DWI) volume in a setting of acute ischemic stroke.

Methods and Materials: Eight experiments were conducted in a pre-clinical middle cerebral artery occlusion (MCAO) model. IVIM and dynamic susceptibility contrast (DSC) imaging were acquired 2.5hr post-MCAO. IVIM was post-processed using software written in-house to produce parametric images of local qCBF, Water Transport Time (WTT), diffusion, and subsequently, PWI/DWI mismatch. These IVIM image parameters were compared with delay-and-dispersion-corrected "local-AIF" DSC perfusion image parameters including Tmax, qCBF, mean transit time (MTT), and mean diffusivity for DSC PWI/DWI mismatch. Final infarct volume was measured 4hrs post-occlusion.

Results: Early (2.5hr post-occlusion) DSC qCBF and IVIM qCBF in the diffusion negative MCA territory correlated strongly ($slope = 1.00, p = 0.01, R^2 = 0.69, Lin's\ CCC = 0.71$), and both DSC and IVIM qCBF values negatively correlated with final infarct volume ($R^2 = 0.78, R^2 = 0.61$ respectively). The volume of hypoperfusion measured at 2.5 hours from DSC qCBF and from IVIM qCBF both predicted final infarct volume with good sensitivity and correlation ($slope = 2.08, R^2 = 0.67, slope = 2.50, R^2 = 0.68$ respectively). IVIM PWI/DWI ratio was correlated with infarct growth ($R^2 = 0.70$) and WTT correlated with MTT ($slope = 0.82, R^2 = 0.60$).

Conclusions: IVIM qCBF correlated strongly with local-AIF DSC qCBF and IVIM PWI/DWI correlated strongly with infarct growth. Both DSC and IVIM quantitative perfusion image acquired early after occlusion were able to predict final infarct volume, and IVIM simultaneous PWI/DWI ratio predicted infarct growth.

Abbr: DSC: dynamic susceptibility contrast, IVIM: intravoxel incoherent motion, qCBF: quantitative cerebral blood flow, WTT: water transport time, MTT: mean transit time, MCAO:

middle cerebral artery occlusion, PWI: perfusion weighted imaging, DWI: diffusion weighted imaging, MD: Mean diffusivity

INTRODUCTION

Acute ischemic stroke occurs when the blood supply to a region of the brain is impeded and the reduction of critical oxygenated blood causes neuronal death. Rapid early intervention by thrombectomy or thrombolysis as soon as possible from symptom onset[1] is effective in treating occlusive disease (MR-CLEAN[2], SWIFT PRIME[3]). However, the DAWN trial suggests the window for safe and effective treatment can be extended for some patients up to 6-24 hours from symptom onset [4], which is crucial for patients with unknown onset time (e.g. "wake up" strokes). Magnetic resonance imaging (MRI) can be used to assess the eligibility for treatment-window extension based on a "mismatch" between the amount of hypoperfused tissue seen in perfusion-weighted imaging (PWI) and amount of irretrievable, dead/infarcted tissue seen in diffusion-weighted imaging (DWI)[5,6] . This "PWI-DWI mismatch" is the operational definition of the ischemic penumbra originally hypothesized in electroencephalogram studies of infarction[7,8]. As such, an accurate measure of this mismatch can be useful in the triage of stroke patients, particularly of those with unknown time of onset, as well as in stroke therapeutic studies.

Ischemic penumbra can be measured by delayed arrival of a contrast bolus[9], which is a measure of tissue perfusion[15]. Tissue distal to an occlusion (even distal to the Circle of Willis) can still receive delayed compensatory oxygenated blood flow delivered through leptomeningeal collateral arteries[10,11], a recent target of neuroprotective therapeutics[12-14]. Inclusion of this compensatory blood flow by using a delay-and-dispersion corrected local-AIF improved the prediction of infarct growth compared to conventional methods[15]. In cases where "late" thrombectomy is being considered, the 'local' quantitative blood supply (qCBF) including blood delivered through collateral arteries, in addition to time from symptom onset and NIH stroke scale, may include valuable information regarding tissue status and infarct development.

This work presents a method of quantifying the penumbral tissue perfusion, including compensatory blood flow, using PWI and DWI simultaneously with intravoxel incoherent motion MRI (IVIM). It compares IVIM prediction to local-AIF dynamic susceptibility contrast MRI (DSC) findings in a well-controlled canine model of acute middle cerebral artery occlusion (MCAO)[16]. We examine qCBF in the tissue-at-risk and the middle cerebral artery territory

against final infarct, and PWI/DWI ratio from DSC Tmax, DSC qCBF, and IVIM qCBF. We demonstrate the potential use of IVIM to quantify cerebral blood flow, water transport time, and perfusion-diffusion mismatch in the tissue-at-risk and the middle cerebral artery territory in a setting of acute ischemic stroke.

METHODS AND MATERIALS

Theory

The mathematics of conventional DSC perfusion analysis results in an overestimation of hypo-perfusion in a setting of robust collateral supply. Use of a local-AIF as a voxel-wise input function corrects for the delay and dispersion that occurs when the bolus of contrast passes through the pial collateral network prior to filling the capillaries in the affected territory[17,18]. With a local-AIF generated for every voxel, rather than a conventional AIF in a brain-feeding artery, the DSC qCBF captures all perfusion in a voxel[15].

Theoretically, IVIM derived tissue qCBF in the PWI-DWI mismatch region should be comparable to local-AIF DSC qCBF and include the local perfusion that conventional DSC does not capture. IVIM is intravoxel, and separates different speeds of diffusion into blood (pseudo-diffusion) and tissue diffusion *within* a voxel independent of contrast bolus[19]. Further, the speed of intravoxel pseudo-diffusion can be used to estimate how much time it would take for 50% of the original capillary molecules in a volume to diffuse out[20]. Therefore, local-AIF DSC and IVIM should be sensitive to the motion of blood in capillaries, whether supplied antegrade or retrograde through the collaterals network without needing to correct for bolus delay[15,21].

Pre-clinical Canine Model

All experiments were conducted using a previously reported preclinical canine model of ischemic stroke[16](Appendix A1. Stroke Model). The two-day experimental protocol was approved by the [BLINDED FOR REVIEW] Institutional Animal Care and Use Committee and reported in compliance with ARRIVE guidelines. The [BLINDED FOR REVIEW] is an AAALAC International accredited institution adhering to the following guidelines, regulations, and policies: a) Guide for the Care and Use of Laboratory Animals (National Research Council), b) USDA Animal Welfare Act and Animal Welfare Regulations, and c) Public Health Service Policy on Humane Care and Use of Laboratory Animals.

Eight canines (mean age = 3.4±3.9y, mean weight = 25.3±5.0kg, 7 female, 1 male) underwent permanent endovascular MCAO via embolic occlusion coils under fluoroscopic guidance with R/L randomization. M1 occlusion was verified via selective internal carotid and vertebral arteriography[16]. To evaluate a larger range of collateral supply, five of eight subjects underwent flow augmentation (simultaneous pressor and vasodilator norepinephrine and hydralazine) to enhance blood supply through the leptomeningeal collateral network by disruption of cerebral autoregulation[14,22]; treated and untreated subjects were pooled.

MRI Acquisition

MRI was acquired 2.5 hours after occlusion. with a 3T MRI scanner (Ingenia, Philips) head-first, prone position with a 15 channel receive-only coil. Multi b-value DWI for IVIM were collected with 10 b-values (0,111, 222, 333, 444, 556, 667, 778, 889, 1000s/mm2) and 3 orthogonal directions. Scans covered the entire head (2D single shot EPI, TR/TE= 3056/91ms, 50 slices/2mm thick, FOV/Matrix = 224mm/128 or FOV/Matrix 160mm/96, total scan time = 5.5 mins, SENSE Factor=2).

DSC perfusion images (coronal plane, 2D gradient echo, T2*-weighted EPI, FOV/Matrix=160mm/176, 5 slices/6mm thick, TR/TE=500/30, 120 phases, total scan time = 60s) were taken along with rapid 15s T1 maps following the "T1 bookend method" (2D Inversion Recovery (IR) Look Locker, single-shot EPI FOV/Matrix=160mm/176, 5 slices/6mm thick). Gadolinium (Gd)-based contrast agent (Multihance, Bracco, Princeton, NJ, USA) followed by a saline flush (Gd: 3mL at 2mL/s, saline: 20mL at 2mL/s) was injected in forepaw.

Diffusion Tensor Imaging (DTI) for mean diffusivity (MD), analogous to more widely used Apparent Diffusion Coefficient (ADC), was acquired for true infarct volume measurements every 30 minutes post-MCAO to track infarct growth over time[11]. A stack of 50 2D DTI slices was prescribed to cover the entire head (slice thickness= 2mm, FOV =128x128 mm/matrix = 128x128, TR/TE = 2993/83ms, FA = 90°, b-values = 0, 800 s/mm^2, 32 directions).

DSC Analysis

DSC qCBF was post-processed using the well-established T1-bookend method[17,18,23-29] (Appendix A2. T1-Bookend DSC) with a voxel-by-voxel local-AIF. This corrected for the late arrival (delay) and "blunting" (dispersion) of the contrast bolus as it propagated through the

brain[15,18] and has shown improved measurement of compensatory blood supply in the ischemic penumbra (Appendix A3. Delay-and-Dispersion-Corrected DSC). This yielded DSC qCBF (in ml/100g/min) and CBV (in ml/100g). Tmax was calculated as the time at which the residue function reached its maximum after deconvolution with an uncorrected AIF.

DWI Analysis

DWI positive tissue (i.e. infarcted) was defined as MD<0.00057 from the DTI mean diffusivity and final infarct volume was calculated 4hrs post-MCAO[16].

IVIM Analysis

IVIM qCBF (in ml/100g/min) and diffusion (in mm^2/s) values were calculated from the 10 b-values using a two-step segmented fit[30-35]. IVIM D (tissue-diffusion component) was fit on a voxel-wise basis to the second component of the standard IVIM bi-exponential $\frac{S_b}{S_0} = fe^{-bD^*} + (1-f)e^{-bD}$ for b-values>250 s/mm^2. Using the calculated IVIM D, the pseudo-diffusion components, f and D*, were fit to the whole equation using nonlinear least squares. The parameter fD* was quantified as qCBF (in ml/100g/min) with the WTT[20] (Appendix A4. IVIM Water Transport Time). Diffusion positive IVIM was defined as IVIM D<0.000515 [36].

After post-processing, the IVIM images were co-registered and resized to anatomically overlap with DSC qCBF images for region-of-interest comparison. Three consecutive IVIM slices were averaged in analysis to match the coarser DSC slice thickness of 6 mm. Previously reported leave-one-out cross validation *T2* map thresholds[20,37], D^* >0.10 s/mm^2 and f >0.30 [21,38] were excluded to remove cerebrospinal fluid (CSF) dominated voxels and minimize partial volume effects without use of a *T2*-prepared IR pulse for CSF suppression[35].

qCBF in MCAO Territory and Final Infarct

2.5hrs post-occlusion, the occluded MCA territory was defined as tissue that is normally supplied by the occluded (right or left) MCA. The average values of IVIM qCBF and DSC qCBF in this MCAO territory that was not infarcted (i.e. diffusion negative, but in the MCAO territory) were compared to each other via linear regression and Bland-Altman plots. The average DSC and IVIM qCBF in the diffusion negative MCAO territory were also used to predict final infarct

volume by linear regression. All analyses were performed in three consecutive 6 mm coronal slices starting at, and posterior to, the M1 segment for both DSC and IVIM images.

Early Hypoperfused Volume and Final Infarct Volume

The 2.5hr hypoperfused volume was calculated first as the volume of tissue in DSC with qCBF<26ml/100g/min, second as DSC Tmax>1s[15], and third in IVIM analysis as IVIM qCBF<26ml/100g/min. Correlation of these hypoperfusion volumes against the final (4 hr) infarct volume[11] was measured via linear regression. This hypoperfused volume was independent of DWI measurements; it was only based on thresholded qCBF, which could possibly include tissue that was DWI positive (i.e. dead).

Perfusion-Diffusion Mismatch Ratio and Infarct Growth

The PWI/DWI volume ratio was calculated from DSC qCBF, IVIM qCBF, and Tmax values. PWI volume was defined as the hypoperfused lesion volume described above. The DWI positive lesion was defined as MD<0.000574 mm^2/s for DSC qCBF and Tmax, and as IVIM D<0.000515 mm^2/s for IVIM images to capture PWI/DWI using only the IVIM acquisition. The PWI/DWI ratio of the hypoperfused lesion to the DWI positive lesion (core infarct) was compared to the change in infarct volume between the time of the perfusion scan and the final 4hr infarct via linear regression.

Hypoperfusion from Local Temporal Parameters

Volumes of 'hypoperfusion' calculated from slowed transit time MTT from DSC (Appendix A3. Local-AIF DSC) and WTT from IVIM (Appendix A4. Intravoxel Incoherent Motion with Water Transport Time) were generated based on varying thresholds from $1 - 10s$. The volumes from the thresholds were compared to examine correlation and agreement. To reduce the sensitivity to noise, values over 20s were excluded as being "unphysical."

Statistics

Linear regression, Bland-Altman, and Lin's Concordance Correlation Coefficient (Lin's CCC) were used to compare qCBF between DSC and IVIM perfusion methods in the MCA territory. Linear regression was used for correlation between qCBF hypoperfused volumes and DWI final

infarct, and between the 2.5hr PWI/DWI ratio and infarct growth between 2.5 and 4hrs. Paired Wilcoxon signed-rank was used to compare hypoperfusion volumes. The bootstrap z-test was used to estimate effect size for power calculation. All statistical analysis was performed in Python 3.11.4 (Anaconda Inc., 2024) and R (Rstudio 3.6.1, Posit PBC, Boston, MA USA, 2019) with statistical significance determined at the p = 0.05 level.

RESULTS

Perfusion and Diffusion Maps

Representative images of DSC qCBF, IVIM qCBF maps, IVIM D, and MD infarct maps acquired 2.5 hrs post-MCAO are shown in Fig.1, with three IVIM slices averaged and resized to match DSC. Subject A was found to have robust collateral supply based on x-ray angiography. The bottom row shows the corresponding images for Subject B with poor collateral supply. Note the pronounced difference in tissue perfusion when tissue is fed by a robust collateral blood supply (Fig.1A vs Fig.1B). In both cases, IVIM qCBF shows similarity with DSC qCBF. The corresponding maps of the IVIM D and mean diffusivity (Fig.1C-D) are also shown. Note that in Subject A the tissue perfusion is reduced (Fig.1A), but tissue viability maintained (Fig.1C), whereas in Subject B both DSC and IVIM imaging showed compromised perfusion (Fig.1B) and a large core infarct (Fig.1D) with minimal salvageable mismatch.

qCBF in the MCA Territory

DSC and IVIM qCBF in the MCA territory strongly correlated (Figure 2A, $R^2 = 0.69, p = 0.01$, $Lin's\ CCC = 0.71$) across collateral status and flow augmentation. Bland Altman showed a significant mean difference (+19ml/100g/min), without bias between DSC qCBF and IVIM qCBF. In comparison, correlation between IVIM qCBF and conventional DSC CBF without inclusion of delayed collateral was weak (R^2=0.16), and linear regression was not significant (p=0.32). Average DSC qCBF and IVIM qCBF in the diffusion negative MCAO territory negatively correlated with final infarct (Figure 2B-C). While both were significant, DSC qCBF demonstrated a stronger correlation than IVIM qCBF.

Hypoperfused Volume Against Final Infarct Volume

Early 2.5hr IVIM hypoperfused volume predicted 4hr infarct volume; larger hypoperfusion correlated with larger final infarct volume (Fig.3). The IVIM qCBF hypoperfusion lesion showed good sensitivity and variance ($slope = 2.50, p = 0.01, R^2 = 0.68$). It performed similarly to DSC qCBF hypoperfusion ($slope = 2.08, p = 0.01, R^2 = 0.67$), while outperforming Tmax hypoperfusion ($slope = 3.29, p = 0.08, R^2 = 0.51$). DSC qCBF showed a mean hypoperfused volume of 2.1±1.1 (range 0.59-4.2), and IVIM qCBF agreed (mean hypoperfused volume= 2.4±0.7 (range 1.5-3.9), Wilcoxon signed-rank p = 0.46). In comparison, conventional DSC showed significantly larger, overestimated, hypoperfused lesion (mean = 3.4±1.3cm^3 (range 1.0-5.8), Wilcoxon signed-rank p = 0.023), and weaker correlation with final infarct volume ($slope = 3.24, p = 0.06, R^2 = 0.46$).

Perfusion-Diffusion Mismatch Ratio and Infarct Growth

The PWI/DWI ratio from Tmax and DSC qCBF showed weak negative correlation with infarct growth (Fig.4A-B). IVIM PWI/DWI ratio returned stronger correlation, potentially due to its ability to capture simultaneous perfusion and diffusion in a single scan and avoiding co-registration or timing mismatch (Fig.4C).

Perfusion Time Parameters

Representative images of Tmax, MTT, and IVIM WTT are shown for the subjects from Fig.1 as parametric images in Fig.5. Thresholding IVIM WTT at 3s returned the strongest correlation against DSC MTT at 3s ($slope = 0.82, p = 0.04, R^2 = 0.60$). One case was left out of analysis but included in the plot as a yellow outlier (Appendix A5. Water Transport Time Correlation). This case highlights the difficulty of fitting IVIM decay to the standard bi-exponential[39], as the curve fit returned low IVIM blood fraction *f* but normal *D** supporting the product *(fD*)* being more accurate than individual parameters[40].

Statistical Power

Regarding power analysis for sample size, the slopes for prediction of final infarct volume using DSC hypoperfusion (Fig.3B) or IVIM hypoperfusion (Fig.3C) did not demonstrate significant difference by the bootstrap z-test (z=-0.55, p = 0.58). R^2 values also did not demonstrate statistically significant difference (z=-0.026, p = 0.98). However, the study was underpowered

due to the sample size, with a minimum requirement of 142 subjects for ideal 80% power of slope.

DISCUSSION

This study demonstrated the sensitivity of IVIM to local compensatory cerebral blood flow, transport time, and perfusion-diffusion mismatch in acute ischemic stroke penumbra. Local-AIF DSC MRI and IVIM MRI, both independently quantified as qCBF in ml/100g/min agreed strongly, and both predicted final infarct volume through qCBF in the diffusion negative MCAO tissue and hypoperfusion lesion volume. The correlation of IVIM qCBF with DSC qCBF supports IVIM as a measure of imaging collateral blood supply in acute stroke[15,21]. Further, our IVIM analysis demonstrates the potential benefit of combining temporal parameters and blood volume into penumbra[41] flow (ml/100g/min) with both DSC qCBF and IVIM qCBF outperforming Tmax for hypoperfusion and PWI/DWI mismatch. As the IVIM is more sensitive to local motion of capillary water, IVIM avoid the complexities of bolus-tracking methods and can yield simultaneous quantitative local perfusion-diffusion mismatch without the need for contrast agent administration.

Imaging the oxygenated blood supplied through the collateral network poses itself as clinically valuable in stroke research and therapeutic studies. The DEFUSE studies demonstrated the value of identifying “a malignant pattern” in triaging patients for thrombectomy[42,43]. Based on the extent of leptomeningeal collateralization identified from xray DSA, the PWI/DWI mismatch may preselect patients with robust collateral supply, precisely the patients who can undergo thrombectomy safely[44]. In acute stroke, blood blocked or delayed by an occlusion is evident as prolonged Tmax or Arrival Time of the bolus in the affected territory. With good collateral supply, the contrast bolus may arrive delayed and dispersed after having traversed the collateral network of small connections and anastomoses and provide vital nutrients and oxygen supply to prevent infarction. We propose this as the reason good collateral supply has been shown to influence endovascular treatment outcome[10] as well as time-to-treatment window[45]. Further, novel neuroprotectant therapeutics designed to further extend the time window for safe intervention have been shown to increase collateral blood supply, and benefit from quantitative rather than relative measurement[13,14,22,46,47].

As shown by Liu et al.[15] accurate assessment of blood supply through a collateral network can be measured with delay-and-dispersion corrected deconvolution analysis of DSC with a local-AIF. Further, Federau et al.[21] proposed IVIM "local perfusion fraction" as a measure of collateral blood supply that conventional DSC could not capture. The correlation of IVIM qCBF to local-AIF DSC qCBF in this current work (Fig.2A) shows that the two methods of measuring "local perfusion" agree and supports IVIM capturing compensatory native and augmented collateral supply in a pre-clinical animal model of acute stroke.

The positive bias in the Bland-Altman analysis of IVIM perfusion and DSC perfusion (Fig.2B) could be due to inclusion of diffusion other than capillary-level blood such as interstitial fluid and cerebrospinal fluid in subarachnoid space; as IVIM is not contrast or spin-labelled, all motion in a voxel will contribute to signal[34,35]. Since Inversion Recovery to suppress CSF will also suppress blood[20,35], instead an automatic T2 threshold was applied instead to remove CSF dominated voxels[20,37], and f and D^* were thresholded. However, partial volume contamination could still lead to overestimation of blood signal. Removal with T2prepared CSF suppression[35] or multi-compartment analysis[48,49] could reduce the offset.

A subject with higher compensatory collateral supply would be expected to have higher average qCBF in the MCAO territory[15], and slower infarct growth[11]. IVIM qCBF in the MCAO territory predicted the final infarct volume; lower perfusion in the diffusion negative MCAO territory correlated with greater final infarct volume similar to DSC qCBF (Fig.2B-C). As the flow augmentation in this study had a dichotomous effect based on original native collateral score[14], the treatment group did not always return a higher penumbral perfusion and smaller final infarct volume.

The PWI/DWI mismatch ratio showed negative correlation with future infarct growth. A higher PWI/DWI ratio 2.5hrs post-occlusion may signal a larger amount of affected tissue getting compensatory flow (i.e. reduced but still delivering vital nutrients and oxygen) and a smaller infarct (Fig.4C). However, there is no guarantee that the collateral supply will be sustained. Interestingly, the PWI/DWI ratio from IVIM measurements outperformed DSC and Tmax in predicting future infarct growth. As IVIM qCBF and DSC qCBF themselves showed strong agreement, the improvement of PWI/DWI with IVIM may be due to IVIM being able to capture simultaneous PWI and DWI, while DSC requires a separate DWI MR sequence. Further

IVIM PWI and DWI have the same FOV and resolution, while Tmax and DSC did not match the DWI dimensions requiring imperfect co-registration.

Significant correlation of WTT and MTT supports IVIM WTT as an estimation of local transit time while the offset highlights limited robustness and the effect of noise in D*. Mathematically, the inverse of D* may return falsely high WTT values when D* is fit to a low value. As the D* parameter alone has shown problems with robustness[50], we only calculated quantitative qCBF as fD^*averaged across an ROI and for calculation of volumes by thresholding; D* was not used as a quantitative value on a voxel-wise basis nor for visual analysis.

Previous work has found correlation between IVIM and DSC[31,33,38] predominately correlating conventional DSC CBV and IVIM *f* which avoids the complications of D* and may be more dependable. However, the correlations seen in our study using IVIM qCBF with WTT against local-AIF DSC qCBF and MTT show improved correlation against local-AIF DSC, value of a time component from IVIM, and use of a more stable D* estimation. Further, IVIM qCBF and PWI/DWI ratio in acute stroke has not previously been compared to DSC qCBF that includes local collateral supply for prediction of final infarct.

The ability to image quantitative longitudinal development of potential penumbra perfusion, track perfusion-diffusion mismatch over time, and study progression of infarction could aid in pre-clinical studies of novel stroke therapeutics. As IVIM is non-contrast, it could capture PWI/DWI mismatch throughout infarct progression without issues of multiple contrast injections[27]. Further, IVIM quantification is independent of qCBF on the normal hemisphere which is critical in studies of novel flow augmentation that may impact the contralateral perfusion[14].

This study is not without its limitations. IVIM is still subject to CSF and interstitial fluid contamination, despite use of a T2weighted-threshold. Use of T2preparation IR pulse[35] or multi-compartment separation of CSF signal during post-processing analysis[48,49] may be of benefit in future studies. Gd-contrast prevented comparison of IVIM and DSC for tracking perfusion-diffusion mismatch throughout infarct progression. An analysis of IVIM qCBF and PWI/DWI mismatch, as the stroke develops over time, would be a worthwhile investigation. Difficulties related to fitting IVIM data and noise prevented voxel-wise comparison to DSC MRI; images were analyzed region-by-region, rather than voxel-by-voxel. The complexities of the model and

physiologic monitoring prevented perfect temporal agreement of DTI, DSC, and IVIM data. Voxel sizes and FOV differed between the two MR sequences preventing perfect co-registration; matching FOV and matrix size may improve correlation. While heartrate and blood pressure were monitored, fluctuations were inevitable. Translation of conclusions derived from animal-based models is a potential limitation, but animal models reduce error in evaluating methods for qCBF calculation with known occlusion time and comparison of subjects at multiple time points under similar physiologic conditions which is not possible in humans. The number of subjects used in this study limits statistical interpretation and significance for ethical considerations. While use of IVIM in stroke triage in the US is limited, a method of imaging repeated PWI/DWI that includes compensatory flow throughout infarct development still has use in pre-clinical research and stroke therapeutics.

CONCLUSION

IVIM qCBF correlated strongly with DSC qCBF, hypoperfusion lesion volume from DSC qCBF and IVIM qCBF predicted final infarct volume, and IVIM simultaneous PWI/DWI ratio predicted infarct growth. As IVIM is a non-contrast method that includes compensatory collateral supply, it poses itself to be a viable candidate for longitudinal measurement of simultaneous perfusion and diffusion in pre-clinical stroke research.

REFERENCES

1. Rehani B, Ammanuel SG, et al. A New Era of Extended Time Window Acute Stroke Interventions Guided by Imaging. *The Neurohospitalist.* 2019;10(1):29-37.
2. Fransen PSS, Beumer D, et al. MR CLEAN, a multicenter randomized clinical trial of endovascular treatment for acute ischemic stroke in the Netherlands: study protocol for a randomized controlled trial. *Trials.* 2014;15(1).
3. Goyal M, Jadhav AP, et al. Analysis of Workflow and Time to Treatment and the Effects on Outcome in Endovascular Treatment of Acute Ischemic Stroke: Results from the SWIFT PRIME Randomized Controlled Trial. *Radiology.* 2016;279(3):888-897.
4. Nogueira RG, Jadhav AP, et al. Thrombectomy 6 to 24 Hours after Stroke with a Mismatch between Deficit and Infarct. *New England Journal of Medicine.* 2018;378(1):11-21.
5. Lansberg MG, Cereda CW, et al. Response to endovascular reperfusion is not time-dependent in patients with salvageable tissue. *Neurology.* 2015;85(8):708-714.
6. Heiss W-D, Zaro-Weber O. Extension of therapeutic window in ischemic stroke by selective mismatch imaging. *International Journal of Stroke.* 2019;14(4):351-358.

7. Leigh R, Knutsson L, et al. Imaging the physiological evolution of the ischemic penumbra in acute ischemic stroke. *Journal of Cerebral Blood Flow & Metabolism.* 2017;38(9):1500-1516.
8. Demeestere J, Wouters A, et al. Review of Perfusion Imaging in Acute Ischemic Stroke. *Stroke.* 2020;51(3):1017-1024.
9. Lansberg MG, Thijs VN, et al. Evaluation of the Clinical–Diffusion and Perfusion–Diffusion Mismatch Models in DEFUSE. *Stroke.* 2007;38(6):1826-1830.
10. Ribo M, Flores A, et al. Extending the Time Window for Endovascular Procedures According to Collateral Pial Circulation. *Stroke.* 2011;42(12):3465-3469.
11. Christoforidis GA, Vakil P, et al. Impact of Pial Collaterals on Infarct Growth Rate in Experimental Acute Ischemic Stroke. *AJNR Am J Neuroradiol.* 2017;38(2):270-275.
12. Christoforidis GA, Saadat N, et al. Effect of early Sanguinate (PEGylated carboxyhemoglobin bovine) infusion on cerebral blood flow to the ischemic core in experimental middle cerebral artery occlusion. *J Neurointerv Surg.* 2022;14(12):1253-1257.
13. Shazeeb MS, King RM, et al. Novel Oxygen Carrier Slows Infarct Growth in Large Vessel Occlusion Dog Model Based on Magnetic Resonance Imaging Analysis. *Stroke.* 2022;53(4):1363-1372.
14. Liu M, Saadat N, et al. Augmentation of perfusion with simultaneous vasodilator and inotropic agents in experimental acute middle cerebral artery occlusion: a pilot study. *J Neurointerv Surg.* 2022.
15. Liu M, Saadat N, et al. Quantification of Collateral Supply with Local-AIF Dynamic Susceptibility Contrast MRI Predicts Infarct Growth. *AJNR Am J Neuroradiol.* 2024;(in press).
16. Christoforidis GA, Rink C, et al. An endovascular canine middle cerebral artery occlusion model for the study of leptomeningeal collateral recruitment. *Investigative radiology.* 2011;46(1):34-40.
17. Jeong YI, Christoforidis GA, et al. Absolute quantitative MR perfusion and comparison against stable‐isotope microspheres. *Magn Reson Med.* 2019;0(0):1-11.
18. Mouannes-Srour JJ, Shin W, et al. Correction for arterial-tissue delay and dispersion in absolute quantitative cerebral perfusion DSC MR imaging. *Magn Reson Med.* 2012;68(2):495-506.
19. Le Bihan D, Breton E, et al. MR imaging of intravoxel incoherent motions: application to diffusion and perfusion in neurologic disorders. *Radiology.* 1986;161(2):401-407.
20. Liu M, Saadat N, et al. Quantitative perfusion and water transport time model from multi b-value diffusion magnetic resonance imaging validated against neutron capture microspheres. *Journal of Medical Imaging.* 2023;10(06).
21. Federau C, Wintermark M, et al. Collateral blood flow measurement with intravoxel incoherent motion perfusion imaging in hyperacute brain stroke. *Neurology.* 2019;92(21).
22. Saadat N, Christoforidis GA, et al. Influence of simultaneous pressor and vasodilatory agents on the evolution of infarct growth in experimental acute middle cerebral artery occlusion. *J Neurointerv Surg.* 2020.
23. Sakaie KE, Shin W, et al. Method for improving the accuracy of quantitative cerebral perfusion imaging. *J Magn Reson Imaging.* 2005;21(5):512-519.

24. Vakil P, Lee JJ, et al. Cerebrovascular occlusive disease: quantitative cerebral blood flow using dynamic susceptibility contrast mr imaging correlates with quantitative H2[15O] PET. *Radiology.* 2013;266(3):879-886.
25. Carroll TJ, Horowitz S, et al. Quantification of cerebral perfusion using the "bookend technique": an evaluation in CNS tumors. *Magn Reson Imaging.* 2008;26(10):1352-1359.
26. Carroll TJ, Rowley HA, et al. Automatic calculation of the arterial input function for cerebral perfusion imaging with MR imaging. *Radiology.* 2003;227(2):593-600.
27. Shin W, Cashen TA, et al. Quantitative CBV measurement from static T1 changes in tissue and correction for intravascular water exchange. *Magn Reson Med.* 2006;56(1):138-145.
28. Shin W, Horowitz S, et al. Quantitative cerebral perfusion using dynamic susceptibility contrast MRI: evaluation of reproducibility and age- and gender-dependence with fully automatic image postprocessing algorithm. *Magn Reson Med.* 2007;58(6):1232-1241.
29. Shah MK, Shin W, et al. Quantitative cerebral MR perfusion imaging: preliminary results in stroke. *J Magn Reson Imaging.* 2010;32(4):796-802.
30. Le Bihan D, Breton E, et al. Separation of diffusion and perfusion in intravoxel incoherent motion MR imaging. *Radiology.* 1988;168(2):497-505.
31. Wirestam R, Borg M, et al. Perfusion-related parameters in intravoxel incoherent motion MR imaging compared with CBV and CBF measured by dynamic susceptibility-contrast MR technique. *Acta Radiol.* 2001;42(2):123-128.
32. Federau C, Maeder P, et al. Quantitative measurement of brain perfusion with intravoxel incoherent motion MR imaging. *Radiology.* 2012;265(3):874-881.
33. Federau C, O'Brien K, et al. Measuring brain perfusion with intravoxel incoherent motion (IVIM): initial clinical experience. *J Magn Reson Imaging.* 2014;39(3):624-632.
34. Federau C, Sumer S, et al. Intravoxel incoherent motion perfusion imaging in acute stroke: initial clinical experience. *Neuroradiology.* 2014;56(8):629-635.
35. Federau C, O'Brien K. Increased brain perfusion contrast with T2‐prepared intravoxel incoherent motion (T2prep IVIM) MRI. *NMR in Biomedicine.* 2014;28(1):9-16.
36. Liu M, Jeong Y, et al. Quantitative CBF and DWI Volume from Single MRI Scan in Stroke. 2021 American Society of NeuroRadiology; 2021.
37. Liu M, Warioba C, et al. Validation and Machine Learning of a New Method for Quantifying CBF with IVIM. American Society of NeuroRadiology Annual Meeting; 2023.
38. Zhu G, Federau C, et al. Comparison of MRI IVIM and MR perfusion imaging in acute ischemic stroke due to large vessel occlusion. *Int J Stroke.* 2020;15(3):332-342.
39. Shazeeb MS, Sotak CH. Limitations in biexponential fitting of NMR inversion-recovery curves. *Journal of Magnetic Resonance.* 2017;276:14-21.
40. Federau C, O'Brien K, et al. Functional Mapping of the Human Visual Cortex with Intravoxel Incoherent Motion MRI. *Plos One.* 2015;10(2).
41. Nael K, Doshi A, et al. MR Perfusion to Determine the Status of Collaterals in Patients with Acute Ischemic Stroke: A Look Beyond Time Maps. *American Journal of Neuroradiology.* 2018;39(2):219-225.
42. Olivot J-M, Mlynash M, et al. Relationships Between Cerebral Perfusion and Reversibility of Acute Diffusion Lesions in DEFUSE. *Stroke.* 2009;40(5):1692-1697.
43. Albers GW, Marks MP, et al. Thrombectomy for Stroke at 6 to 16 Hours with Selection by Perfusion Imaging. *New England Journal of Medicine.* 2018;378(8):708-718.

44. Kim SJ, Seok JM, et al. MR Mismatch Profiles in Patients with Intracranial Atherosclerotic Stroke: A Comprehensive approach Comparing Stroke Subtypes. *Journal of Cerebral Blood Flow & Metabolism.* 2009;29(6):1138-1145.
45. Hwang YH, Kang DH, et al. Impact of Time-to-Reperfusion on Outcome in Patients with Poor Collaterals. *American Journal of Neuroradiology.* 2015;36(3):495-500.
46. Warioba C, Liu M, et al. Efficacy Assessment of Cerebral Perfusion Augmentation Through Functional Connectivity in an Acute Canine Stroke Model. *American Journal of Neuroradiology.* 2024.
47. King RM, Anagnostakou V, et al. Selective brain cooling with a novel catheter reduces infarct growth after recanalization in a canine large vessel occlusion model. *Interventional Neuroradiology.* 2024.
48. Liu M, Dyke J, et al. Quantification of Multi-Compartment Flow with Spectral Diffusion MRI. *Arxiv Phys/Med Phys.* 2024.
49. Wong SM, Backes WH, et al. Spectral Diffusion Analysis of Intravoxel Incoherent Motion MRI in Cerebral Small Vessel Disease. *J Magn Reson Imaging.* 2019;51(4):1170-1180.
50. Wu WC, Chen YF, et al. Caveat of measuring perfusion indexes using intravoxel incoherent motion magnetic resonance imaging in the human brain. *Eur Radiol.* 2015;25(8):2485-2492.
51. Thomsen BB, Gredal H, et al. Spontaneous ischaemic stroke lesions in a dog brain: neuropathological characterisation and comparison to human ischaemic stroke. *Acta Vet Scand.* 2017;59(1):7.
52. McHedlishvili G, Kuridze N. The modular organization of the pial arterial system in phylogeny. *J Cereb Blood Flow Metab.* 1984;4(3):391-396.
53. Suo S, Cao M, et al. Stroke assessment with intravoxel incoherent motion diffusion-weighted MRI. *NMR in Biomedicine.* 2016;29(3):320-328.
54. Gao QQ, Lu SS, et al. Quantitative assessment of hyperacute cerebral infarction with intravoxel incoherent motion MR imaging: Initial experience in a canine stroke model. *J Magn Reson Imaging.* 2016;46(2):550-556.
55. Le Bihan D, Turner R. The capillary network: a link between IVIM and classical perfusion. *Magn Reson Med.* 1992;27(1):171-178.

FIGURES AND TABLES

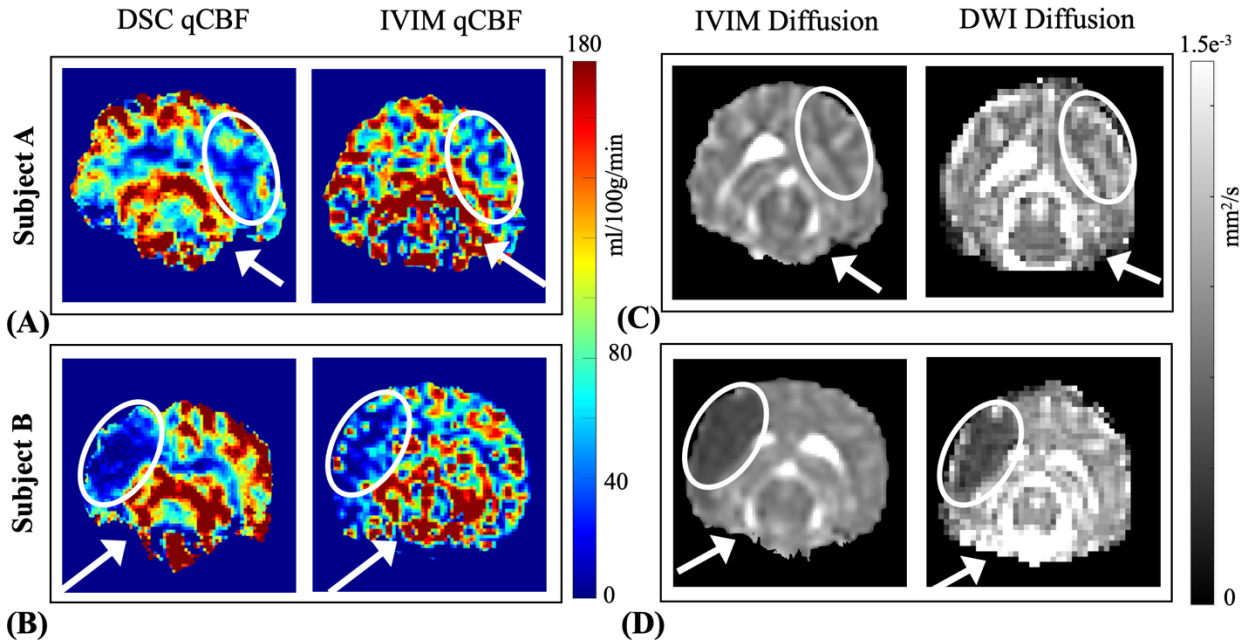

Figure 1. A comparison of qCBF in ml/100g/min between DSC and IVIM for subject A with robust collateral supply (A) and subject B with poor collateral supply (B). DSC were fully quantitative and corrected for arterial delay and dispersion effects, IVIM was quantified with water transport time. The corresponding diffusion maps shown in (C) and (D), respectively. White arrows denote the MCA coil, white ovals denote the MCA territory. IVIM qCBF is averaged across three slices to match the 6mm slice thickness of DSC, and along with an automatic T2 threshold, voxels with D*>10 and/or f > 0.30 are excluded to remove fast-flowing CSF-dominated voxels.

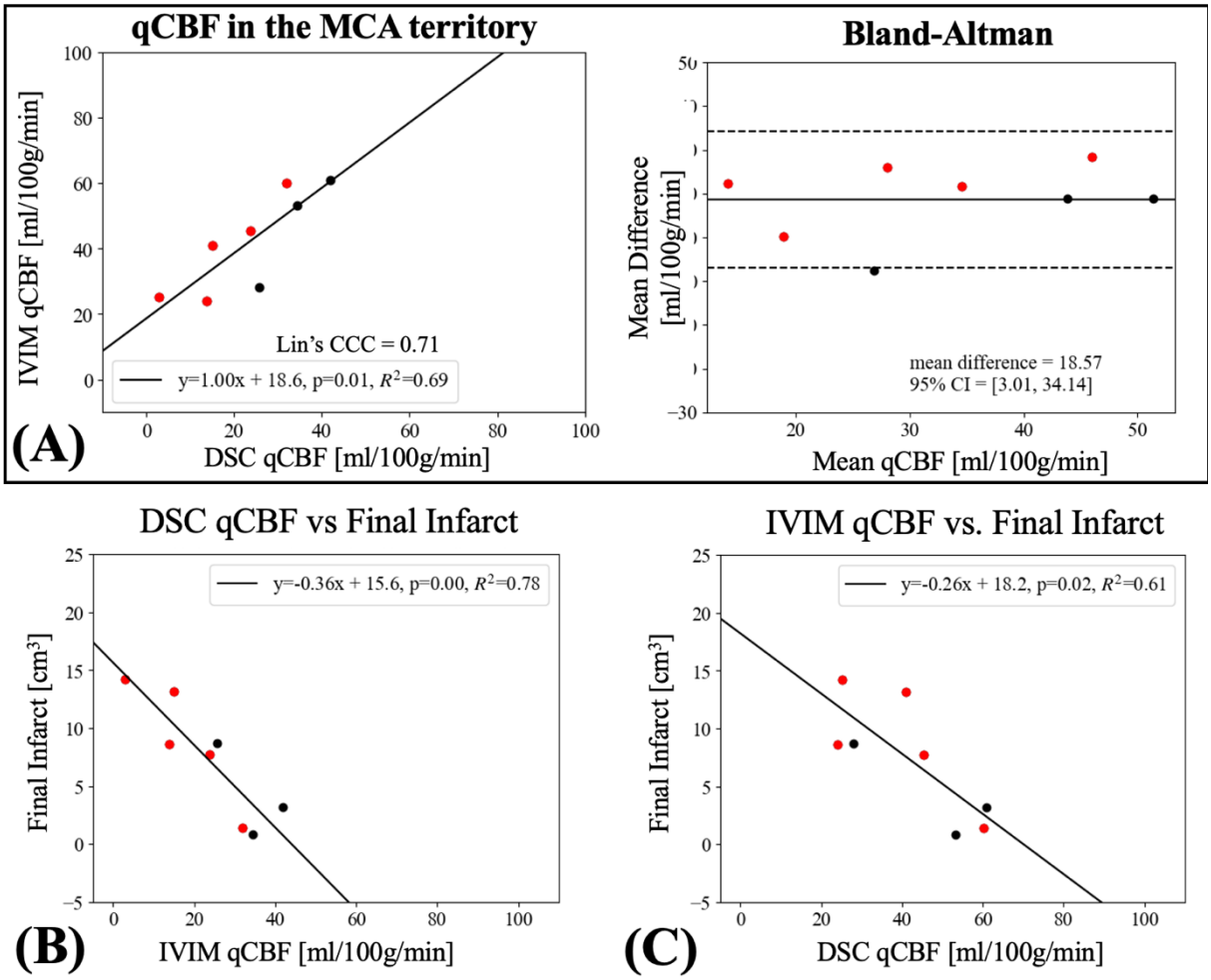

Figure 2. (A) Correlation and linear regression of IVIM qCBF against DSC qCBF in the diffusion negative MCA territory 2.5 hours post MCAO with corresponding Bland-Altman plot. Final (4 hour) infarct volume correlated against (B) DSC qCBF and (C) IVIM qCBF. Experiments were pooled over treatment and baseline collateralization to expand range of collateral supply. Red represents those that received flow augmentation treatment.

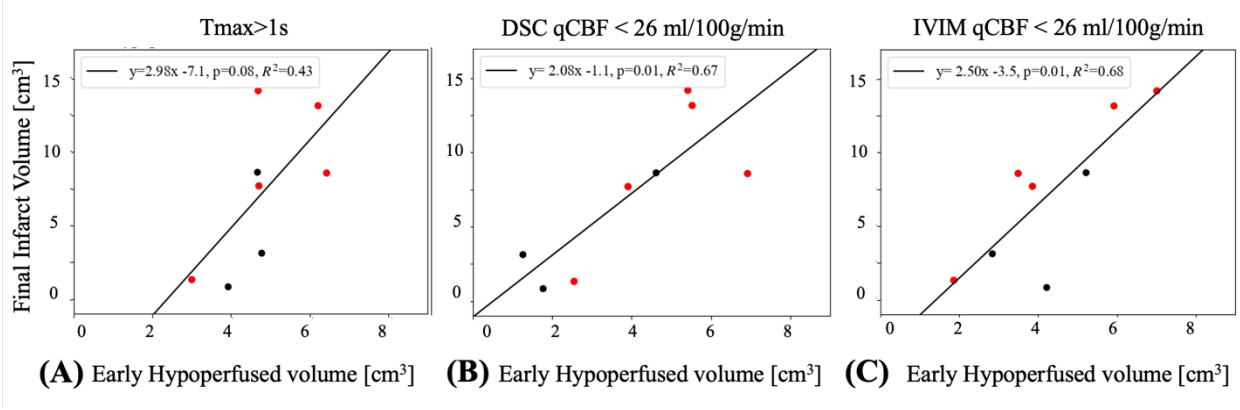

Figure 3. The hypoperfused lesion volume at 2.5 hours post MCAO was a predictor of final infarct volume for hypoperfusion defined as (A) Tmax>1s, (B) DSC qCBF < 26 ml/100g/min and (C) IVIM qCBF <26 ml/100g/min. Experiments were pooled over treatment and baseline collateralization to expand range of collateral supply. Red represents those that received flow augmentation treatment.

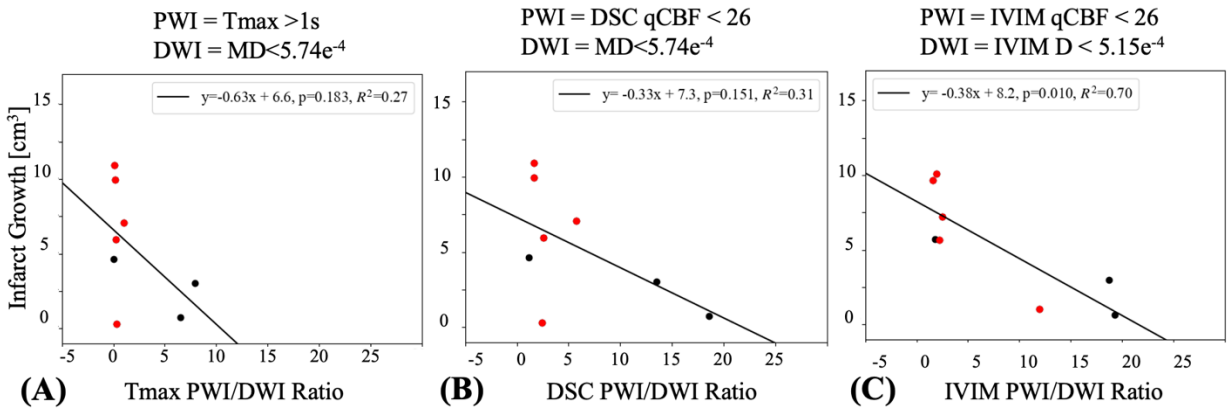

Figure 4. The PWI/DWI ratio of hypoperfused lesion to diffusion positive core at 2.5 hours post MCAO correlated against the infarct growth between the perfusion scan and the final 4-hour infarct. The PWI lesions are defined by thresholding (A) Tmax, (B) DSC qCBF, and (C) IVIM qCBF. The DWI lesions are defined by (A, B) coregistered mean diffusivity and (C) IVIM D. Experiments were pooled over treatment and baseline collateralization to expand range of collateral supply. Red represents those that received flow augmentation treatment.

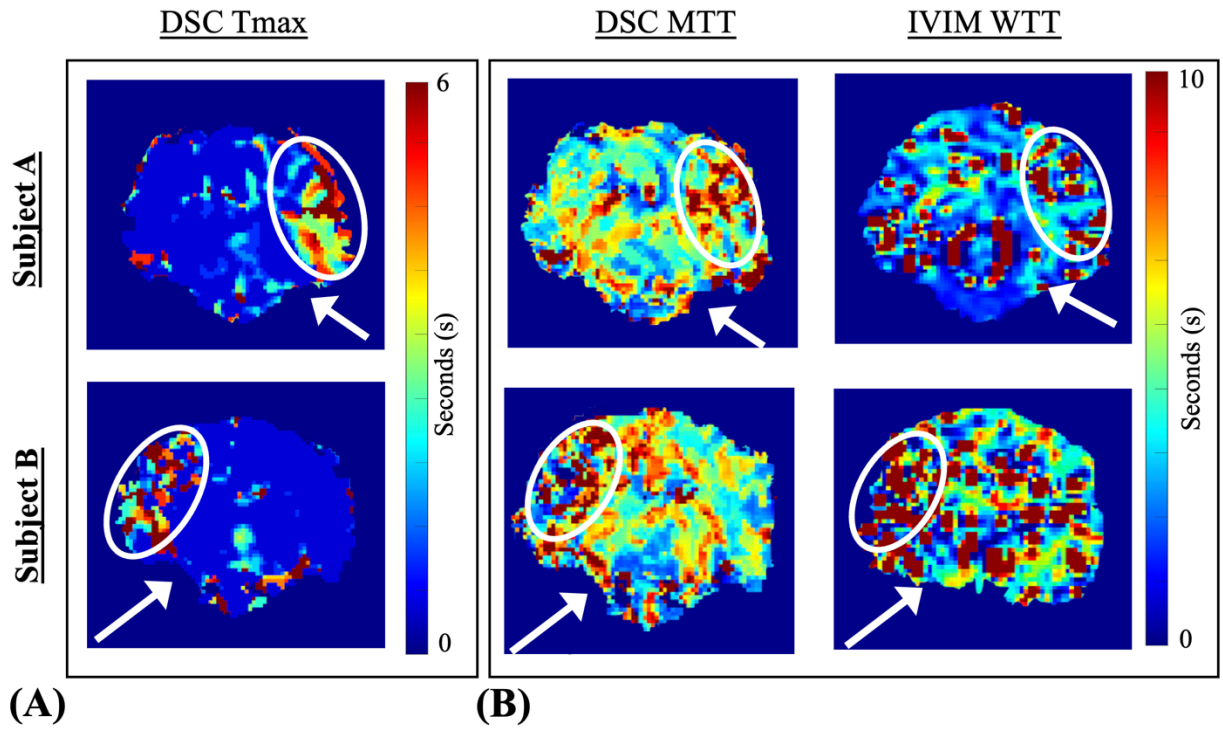

Figure 5. Representative images of (A) Tmax, and (B) MTT and IVIM WTT for the same Subject A (top row, good collaterals) and Subject B (bottom row, bad collaterals) from Figure 1. Tmax is calculated from DSC prior to delay and dispersion correction to capture the delayed arterial bolus. MTT is calculated from DSC after delay and dispersion correction to capture local perfusion speed. WTT is the inverse of D* and represents the intravoxel diffusion speed. White arrows denote the MCA coil, white ovals denote the MCA territory. To reduce the fitting sensitivity as the inverse of D*, WTT values over 20s were removed from consideration

APPENDIX

A1. Stroke Model

All experiments were conducted using a preclinical canine model of ischemic stroke[16]. The two-day experimental protocol was approved by the University of Chicago Institutional Animal Care and Use Committee and reported in compliance with ARRIVE guidelines. Canines have a gyrencephalic neocortex with similar ratio of white to grey matter as well as comparable pial arteriolar network organization critical in modeling collateral arterial blood supply and predicting infarct evolution[51,52].

The canine model has several advantages as a model for assessment of infarct progression using perfusion and diffusion imaging studies. The neurovascular structure of

canines also allows a range of endovascular devices and interventional radiology techniques allowing minimal invasion with real-time visualization of occlusion, preventing imaging artifacts and traumatic cerebrovascular reaction from open surgical occlusion and is a relatively inexpensive alternative to nonhuman primate models of acute ischemia.

Animals underwent permanent endovascular middle cerebral artery occlusion (MCAO) via embolic occlusion coils at the M1 segment with R/L randomized throughout the experiments. Vertebral and bilateral internal carotid arteriograms confirmed MCAO without involvement of other vessels and assessed pial collateral recruitment. Subjects underwent arteriography and all CBF assessment under general anesthesia. Isoflurane (1% End-Tidal, 0.75 minimum alveolar concentration for canines), propofol infusion (6 mg/kg IV followed by continuous 0.1-0.2 mg/min), and intravenous rocuronium (0.4-0.6 mg/kg every 10-30 minutes) were used to maintain anesthesia with minimal influence on cerebral perfusion. Physiology was monitored via invasive blood pressure, End-Tidal CO_2, O_2 saturation, rectal temperature, heart rate, cardiac rhythm, arterial blood gases, glucose, electrolytes, and hematocrit. Animals were euthanized either the same evening or the following day. Those with unanticipated events such as abnormal baseline MRI, intraprocedural intracranial vessel perforation, or excessive deviation in physiologic parameters during MCAO (presumably from an unanticipated procedural related event) were excluded from this study. This current study analyzed only successful controls and flow augmentations subjects of the parent study with completed DSC, IVIM, and DTI sequences. Throughout experiments physiologic parameters were maintained within normal range, excluding blood pressure for experiments involving flow augmentation.

A2. T1-Bookend DSC qCBF

When contrast is injected via IV, it travels through the heart and lungs and finally to the circle of Willis before perfusing the brain. In dynamic susceptibility contrast MRI, the shape of contrast bolus upon entering the brain represents the Global-AIF. When this Global-AIF signal is fit to appropriate mathematical models, parameters of interest such a cerebral blood flow, cerebral blood volume, and mean transit time are extracted [26]. The volume of blood in a voxel is proportional to the area under the tissue concentration curve during the first pass of contrast divided by the area under the pure blood curve.

$$\mathrm{rCBV} \propto \frac{\int [\mathrm{Gd}](t)dt}{\int \text{Global-AIF}(t)dt} \quad (1)$$

To calculate blood flow, the tissue capillary bed can be modeled as a linear system and the AIF can be modeled as a sum of time-shifted and scaled Dirac delta function inputs. The fraction of injected Gadolinium contrast (Gd) in the tissue at time t after the delta input is the residue function, R(t). As the AIF is not instantaneous, it is instead dispersed in time as a narrow curve. This curve can be represented as a set of dirac delta functions at different time delays, i.e. a convolution of the AIF with the residue function.

$$[\mathrm{Gd}](t) = \mathrm{CBF} \times \text{Global-AIF}(t) \otimes R(t) \tag{2}$$

Once the Global-AIF is chosen there are two unknowns, meaning the residue function scaled by CBF is determined by deconvolution via single value decomposition. Mean transit time (MTT), i.e. the average time a particle traveled through the tissue bed, can then be calculated from the residual.

$$\mathrm{rCBF} \propto \max\big(\mathrm{CBF} \times R(t)\big) \tag{3}$$

$$\mathrm{MTT} = \int R(t) \tag{4}$$

Absolute quantification in ml/100g/min with delay and dispersion corrections is applied via the T1 bookend method[18,24-29]. The DSC scan is bookend-ed by T1 mapping sequences to reduce sensitivity of DSC to AIF selection. Steady-state CBV (qCBV) is calculated using the pre and post T1 maps and used as a calibration factor[23]

$$\mathrm{qCBV} = \frac{\left(\frac{1}{\mathrm{T1_{post}}} - \frac{1}{\mathrm{T1_{pre}}}\right)_{\mathrm{tissue}}}{\left(\frac{1}{\mathrm{T1_{post}}} - \frac{1}{\mathrm{T1_{pre}}}\right)_{\mathrm{blood}}} \tag{5}$$

Water exchange correction factors (WCF) can be determined to account for the residual gadolinium in the blood pool[27] a function of change in T1 of blood (R_1)

$$\mathrm{WCF} = 0.35\Delta R_1^2 + 0.11\Delta R_1 + 0.06 \tag{6}$$

Combining these returns quantitative cerebral blood flow from conventional DSC.

$$\mathrm{qCBF_{Global\text{-}AIF}} = \frac{1}{\rho}\left(\frac{1-\mathrm{Hct_{LV}}}{1-\mathrm{Hct_{SV}}}\right)\left(\frac{\mathrm{qCBV_{SS,WM}}}{\mathrm{rCBV_{DSC,WM}}}\right) \times \mathrm{rCBF_{Global\text{-}AIF}} \times \mathrm{WCF} \tag{7}$$

Here $\mathrm{rCBF_{Global\text{-}AIF}}$ is the relative CBF calculated from standard deconvolution of the voxel contrast curve deconvolved from the Global-AIF, $\mathrm{rCBV_{DSC,WM}}$ is the average relative white matter CBV from the DSC images, $\mathrm{qCBV_{SS,WM}}$ is the average white matter steady-state CBV

quantified using the T1 maps, and WCF as the water exchange correction factor. ρ is the average density of brain tissue (1.04 g/ml), and $\mathrm{Hct_{LV}}$ and $\mathrm{HCT_{SV}}$ are the hematocrit levels in large (0.45) and small vessels (0.25), respectively. With this we now have quantitative values for all terms in the central volume principal:

$$\mathrm{qCBF\ (ml/100g/min)} = \frac{\mathrm{qCBV\ (ml/100g)}}{\mathrm{MTT\ (min)}} \tag{8}$$

A3. Local-AIF DSC

When there is an occlusion of a major artery, blood will have to travel around the occlusion to reach the infarcted hemisphere (Figure A3). The delay and the dispersion as blood travels through the collateral network can be corrected for with a Local-AIF to include collateral supply as shown by Liu et al., (2024)[15]. With a selection of the Global-AIF based on automatic early arrival time and narrow bolus, and selection of VOF in the sagittal sinus, the strength of delay and dispersion based on arrival time can be calculated as α and β as a function of the time delay $\mathrm{t_D}$ between Global-AIF and VOF.

$$\mathrm{VOF}(\mathrm{t}+\mathrm{t_D}) = \frac{\alpha}{(\mathrm{t_D}+1)}\,\mathrm{e}^{-\frac{\beta \mathrm{t}}{\mathrm{t_D}}} \otimes \mathrm{Global\text{-}AIF}(\mathrm{t}) \tag{9}$$

Delay is corrected for as the delay of bolus arrival time to local voxels compared to the Global-AIF. Dispersion is corrected for by comparing the bolus shape of the AIF to that of venous outflow at the sagittal sinus. The Local-AIF for every voxel with a voxel-specific delay of Δt can be found by deconvolving the Global-AIF and the residue function of the VOF using the fit parameters α and β from Eq. 9

$$\mathrm{Local\text{-}AIF}(\mathrm{t}) = \mathrm{Global\text{-}AIF}(\mathrm{t}-\Delta\mathrm{t}) \otimes \frac{\alpha}{(\Delta\mathrm{t}+1)}\,\mathrm{e}^{-\frac{\beta \mathrm{t}}{\Delta \mathrm{t}}} \tag{10}$$

This local-AIF now corrects for delayed arrival time (Δt) and bolus dispersion ($\otimes\ \mathrm{e}^{-\frac{\beta \mathrm{t}}{\Delta \mathrm{t}}}$). Further, the correction term approaches unity at Δt approaches 0, recovering the Global result in the absence of delayed and dispersed collateral supply[15]. Replacement of the Global-AIF in Eq. 2 and Eq. 7 with the Local-AIF that has delay and dispersion correction will return Local-AIF perfusion that includes collateral supply and retrograde flow distal to an occlusion.

$$[\mathrm{Gd}](\mathrm{t}) = \mathrm{rCBF_{Local\text{-}AIF}} \times \mathrm{Global\text{-}AIF}(\mathrm{t}) \otimes \frac{\alpha}{(\Delta\mathrm{t}+1)}\,\mathrm{e}^{-\frac{\beta \mathrm{t}}{\Delta \mathrm{t}}} \otimes \mathrm{R}(\mathrm{t}) \tag{11}$$

$$\mathrm{qCBF_{Local\text{-}AIF}} = \frac{1}{\rho}\left(\frac{1-\mathrm{Hct_{LV}}}{1-\mathrm{Hct_{SV}}}\right)\left(\frac{\mathrm{qCBV_{SS,WM}}}{\mathrm{rCBV_{DSC,WM}}}\right) \times \mathrm{rCBF_{Local\text{-}AIF}} \times \mathrm{WCF} \qquad (12)$$

Quantitative perfusion calculated with this method of Local-AIF DSC has been shown to correlate strongly with pial collateral supply from angiography and infarct growth[15]. Mean transit time can then be calculated from the residual with qCBF with $\mathrm{qCBF_{Local\text{-}AIF}}$ in Eq.4 in Appendix 2.

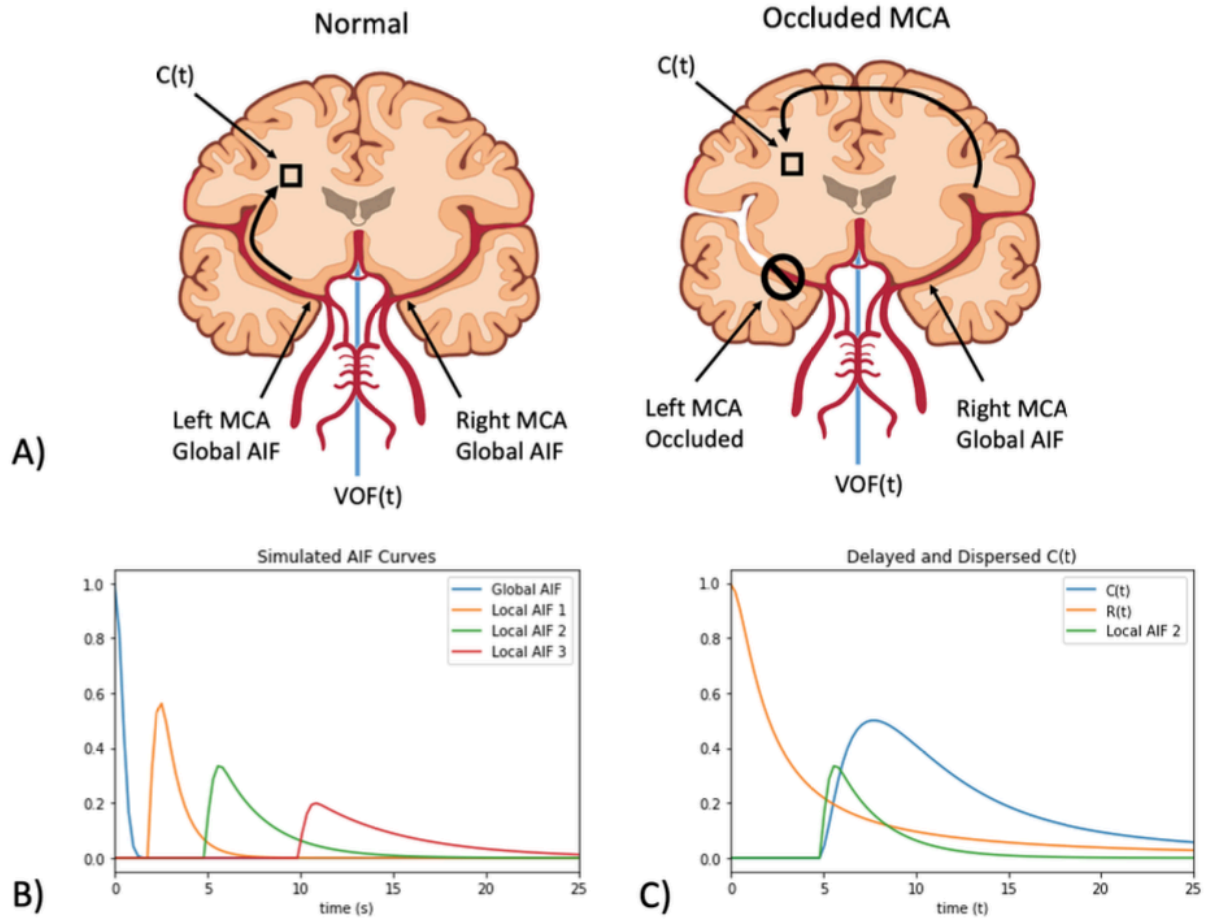

Figure A3. Demonstration of Delay and Dispersion effects. A) comparison of blood pathway through the brain from the MCA for a normal (left) and an occluded (right) MCA. B) Examples of simulated local-AIF curves with increasing delay and increasing dispersion. These would be local-AIFs for voxels at increasing distances from the normal hemisphere in A). C) The effect of a delayed and dispersed local-AIF on a contrast curve. If one assumed the global AIF and deconvolves the contrast curve C(t), the Residue function R(t) would be artificially delayed and dispersed due to the longer path. Correction of the delay of contrast arrival will allow inclusion of compensatory perfusion that reaches the occluded hemisphere through the collateral network, rather than through the MCAs. From Liu, M. (2024) *Use, Optimization, and Expansion of Quantitative Magnetic Resonance Perfusion Imaging in Cerebrovascular Disease* [Doctoral Dissertation, University of Chicago]. doi:10.6082/uchicago.7506.

A4. Intravoxel Incoherent Motion with Water Transport Time

Intravoxel incoherent motion (IVIM) is a non-contrast MRI is derived from multi b-value diffusion weighted imaging (DWI) and sensitive to intravoxel motion of water in the brain. Unlike DSC which measures hypoperfusion based on a smaller and delayed bolus imaged in a voxel, hypoperfusion with IVIM is measured from *intravoxel* motion, so captures local flow without a need to correct for delayed or dispersed bolus from a major artery. As such, IVIM does not suffer from inaccuracies from AIF selection and can reflect local capillary perfusion within the ischemic penumbra in acute stroke[21,34,53,54]. In IVIM, lower b-values are sensitive to fast diffusion such as perfusing blood, whereas higher b-values probe much slower interstitial water[19,30]. This means that the standard mono-exponential for standard DWI apparent diffusion coefficient (ADC) is expanded into a bi-exponential.

$$\frac{S(b)}{S(0)} = fe^{-bD^*} + (1-f)e^{-bD} \tag{13}$$

In the standard two-compartment model the first term measures the fraction of signal in a voxel that is blood (f), and its pseudo-diffusion coefficient D^*. The second term represents the remaining signal due to interstitial tissue diffusion $(1-f)$ and the tissue diffusion coefficient (D). Using the multi-compartment Gaussian water transport model derived recently by Liu et al., (2023) returns "Water Transport Time" (analogous to MTT) from the IVIM signal and quantified cerebral blood flow in ml/100g/min[20]. WTT can be solved for by integrating over a 3D sphere and solving for time t at which 50% of the initial molecules have diffused out of the unit sphere.

$$\frac{4\pi}{\left(\sqrt{4\pi D^* t}\right)^3}\int_{0mm}^{.5mm} e^{-\frac{r^2}{4D^*t}} r^2 dr = 0.50 \tag{14}$$

$$WTT = \frac{(.32mm)^2}{2D} \tag{15}$$

With assumed values of $\rho = 1.04 g/mL$ and water content fraction $f_w = .79$, this can be plugged into the central volume equation to return perfusion in ml/100g/min as

$$qCBF_{WTT} = \frac{CBV}{WTT} = \frac{f \times f_w}{\rho}\frac{2D^*}{(.32)^2} = fD^* \times \frac{2f_w}{\rho(.32)^2} \approx fD^* \times 93000 \tag{16}$$

As IVIM is based on a multi-b-value acquisition, it also includes high b-values nominally used identification of the infarcted core. Therefore, by acquiring multiple b-values, a DWI acquisition

can capture simultaneous ADC ***and*** quantitative tissue perfusion[30,48] independent of capillary geometry assumptions[55]. Intravoxel motion rather than AIF deconvolution avoids falsely underestimated perfusion due to delayed and dispersed contrast-agent or spin-labelling and therefore should also include compensatory collateral supply like Local-AIF DSC.

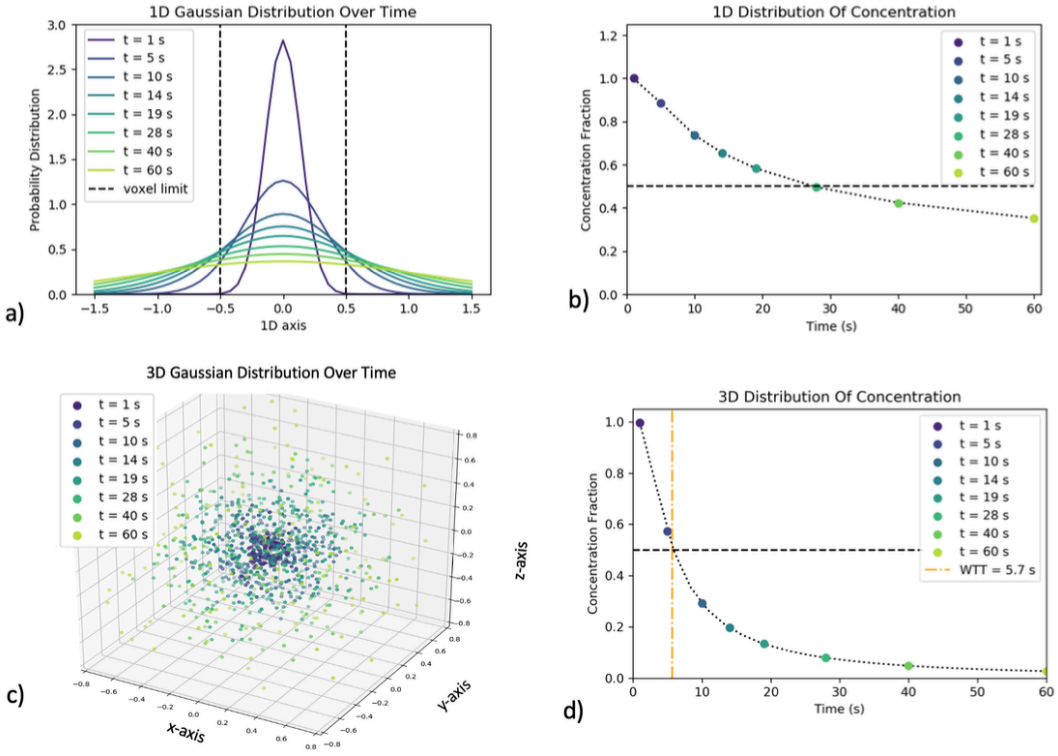

Figure A4. An example of diffusion from 1D and 3D gaussian random walk colorcoded as distributions over time. a) Demonstrates the change in the 1D probability density function as a function of time, assuming an instantaneous random walk from the center of the voxel, where a voxel is a range along a single line. b) Demonstrates the change in the concentration in the 1D voxel as a function of time, as expected as particles diffuse, the concentration drops. c) Demonstrates the change in the 3D density as a function of time, where the voxel would be within the limits of -0.5mm and 0.5mm on all three axes to represent the 1mm unit sphere. d) Demonstrates the change in that 3D concentration as a function of time from isotropic diffusion. This drop in concentration as the original molecules diffuse out of the sphere is what causes the signal decay in MRI DWI. From Liu, M. (2024) *Use, Optimization, and Expansion of Quantitative Magnetic Resonance Perfusion Imaging in Cerebrovascular Disease* [Doctoral Dissertation, University of Chicago]. doi:10.6082/uchicago.7506.

A5. Water Transport Time Correlation

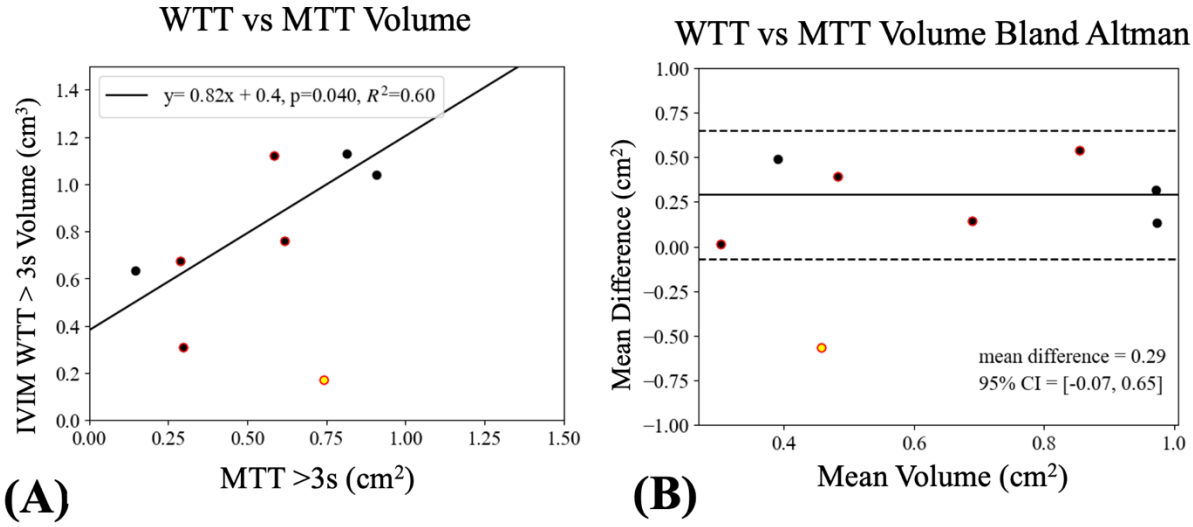

Correlation of (A) MTT>3s volume against IVIM WTT>3s volume. (B) Bland-Altman between MTT and WTT. MTT and WTT represent the mean transit time within a voxel meaning thresholded at 3s represents tissue that is perfusing slowly. Colored yellow is one outlier where the IVIM map had *f* close to zero but normal *D** values that did not indicate slower flow meaning WTT was not heightened. The segmented fit returned low IVIM blood fraction *f* but normal *D**, demonstrating the IVIM parameter product (*fD**) being more accurate than individual parameters, also observed in other work[40].